i-ETC: ISEL Academic Journal of Electronics, Telecommunications and Computers
CETC2011 Issue, Vol. 2, n. 1 (2013) ID-10

Room Temperature Photoluminescence and Photoconductivity of Wet Chemical Deposited ZnO Nanowires Used for Solar Cells

S.R. Bhattacharyya, R. Ayouchi, J. Pereira and R. Schwarz
Department of Physics & ICEMS, Instituto Superior Técnico, Lisbon, Portugal
soumya.bhattacharyya@ist.utl.pt

Keywords: ZnO nanowires, wet chemical process, transport properties, TPC, PL.

Abstract: ZnO 1-D nanostructures (nanowires) were deposited by a two-step wet chemical process. The dimensions of wires were about 100 nm - 1100 nm in length and about 20 - 120 nm in diameter. Scanning electron microscopy (SEM) and X-ray diffraction (XRD) technique was used to obtain the microstructural information from the films. The nanowire films were also characterized optically by transmittance measurement and room temperature photoluminescence (PL) measurements. The transport properties of the samples were characterized by performing transient photoconductivity (TPC) experiments.

1 INTRODUCTION

In the attempts to tap the unconventional energy resources by utilization of solar emission as a clean source of energy, during the last 30 years, there has been a steady progress from silicon-based solar cells to quarternary chalcogenide based compound semiconductor solar cells [1]. But the main bottleneck in this regard has been its efficiency [1], which has seldom crossed the double-digit figure and has thus proved detrimental for adaptation by industry for wider marketing. The latest attempt to break this throttle in regards to solar cell deficiencies has been the utilization of organics and dyes for fabrication of cheap and efficient organic solar cells and dye sensitized solar cells (DSSC). Along with the organic solar cell technology [2], the DSSC research also seems promising [3].

One of the main components of a DSSC is nanoparticles of a wide direct band gap semiconductor, like titanium oxide (TiO_2) or zinc oxide (ZnO) for enhanced light capture and scattering within the cell to increase its efficiency.

In conventional nanoparticle-based DSSCs, the electrons move through the electrolyte to reach the electrode passing within the nanoparticles by percolation or hopping mechanism. With each hop, the electron can recombine with the electrolyte. Under this condition, the diffusion is slow and thus the efficiency of the cell is limited by the recombination. However, ZnO nanowire DSSCs provide a direct path to the anode, which increases the diffusion rate, hence its mobility, without increasing the recombination rate; the other advantages of using nanowires being lower reflective losses and intensive light trapping within the solar cell structure [4]. This could prove important for increasing the solar cell efficiency. But in order to put it into optoelectronic device application, it is imperative to have clear idea about the optical and transport properties of the nanowires.

Apart from its application in DSSC, ZnO nanowires has demonstrated potentiality in the field of energy harvesting through harnessing its piezo-electric property- to convert mechanical energy to electrical energy. This constitutes an alternative application of semiconducting material for energy production and is currently a very hot topic of research [5,6].

In this communication we present our results on the microstructural, optical and transport

properties of the ZnO nanowires grown by two-step wet chemical technique.

2 EXPERIMENTAL PROCEDURE

The ZnO nanowire films were deposited by a simple two-step wet chemical technique on Corning glass substrates. The initial seeding layer with a thickness of about 50 nm was deposited onto the glass substrate by pulsed laser deposition (PLD) technique using solid ZnO (purity 99.999%) target. For the deposition, the 2nd harmonic line at 532 nm of a Q-switched Nd:YAG pulsed laser was used. The 5 ns duration pulses were shot at the target at the rate of 5 Hz. The plasma plume formed by the laser hitting the target produced a homogeneous and consistent film with the particle size of about 10 nm, at a deposition rate of about 2 nm/min. Prior to deposition; the system was evacuated to a base pressure of 10^{-7} mbar. The deposition was carried out in oxygen atmosphere with a system pressure of 10^{-2} mbar. The substrate temperature was kept at 673 K and the target to substrate distance was fixed at 5 cm. The as-deposited films were used as seeding layer for the wet chemical deposition of nanowires.

The chemical deposition of nanowires on top of the seed layer was carried out in aqueous medium using varying ratio R (1:10, 1:20, 1:30, 1:35 and 1:40) of zinc nitrate ($Zn(NO_3)_2.6H_2O$) as zinc containing precursor and sodium hydroxide (NaOH). All the chemicals were reagent grade. The depositions were carried out for 90 minutes at 333 K in a magnetic stirrer at a stirring speed of 500 rpm to obtain films with nanowires of different aspect ratio. For the depositions, the samples were immersed vertically into a 100 ml beaker containing 40 ml of aqueous solution with the two precursors mixed proportionately. After the deposition, the substrates were removed and deionized distilled water was trickled from the back side to wash away any excess residues and the films were subsequently dried in air at 350 K for 15 minutes before being utilized for further characterizations.

The microstructure of these nanowires were studied by scanning electron microscopy (SEM), while the crystal orientation and structure was verified from X-ray diffraction (XRD) scans in the θ-2θ mode. The optical transmittance and reflectance for the films was measured at room temperature using a Jobin-Yvon UV-VIS-NIR spectrophotometer. Additionally, steady-state PL was performed on these samples at room temperature (300 K) to obtain defect related information. The PL measurement was carried out using a 325 nm HeCd laser (10 mW power) to excite the ZnO samples. Photoluminescence from the sample was directed into a monochromator and collected by a photomultiplier for the preset wavelength range. The signal was then fed into a dual-phase Stanford Research SR830 lock-in amplifier, which was interfaced with the computer by Labview 8 for automatic data acquisition. A chopper was placed in the beam path and set at 19 Hz frequency to produce a chopped (a.c.) signal. A 475 nm cut-off filter was used to suppress the first and the second order laser line from the spectra. The transport properties of the films were investigated by transient photocurrent measurements.

For the transient photocurrent-response (TPC), a 266 nm UV line of Q-switched Nd:YAG laser, shooting 5 ns pulses at ~ 2 mJ/cm^2, with a repetition rate of 5 pulses/second and a spot size of 1 mm diameter was used. The measurements were carried out with coplanar aluminium contacts deposited on the films. The current generated was dropped along a variable shunt resistance ranging from 50 Ω to 1 MΩ, as selected for different time windows, and the corresponding signal was measured with a Tektronix 200 MHz bandwidth digital oscilloscope. It was later converted into current for further calculations, with proper zero corrections. The applied voltage on the samples was 15 V and the photocurrent decay was measured in several time windows ranging from 500 ns to 100 μs. Below the 500 ns time scale, the decay signal was too weak to capture.

3 RESULTS AND DISCUSSIONS

The nanostructure of the ZnO layers was studied using a Jeol 7001F SEM. Figs. 1 (a-e) show the representative SEM micrographs of the ZnO nanostructures for the films Z1, Z2, Z3, Z4 and Z5 deposited with R as 1:10, 1:20, 1:30, 1:35 and 1:40, respectively. The sample Z1 deposited with R = 1:10 showed very nascent tendency for 1-D growth, with the morphology representing dwarf stubs, with arrested vertical growth. Also for the sample Z2, the nanostructures formed aggregated clusters with nanoflower like feature, with each of the nanostructures constituting the "petals" which were broader at the centre and pointy towards the tips. They showed arrested vertical elongation. But for samples Z3, Z4 and Z5, definite 1-D growth in the vertical direction was observed with their lengths (in these cases) being much larger than their diameters. Since our aim was growth of vertically

aligned nanowires only the samples Z3, Z4 and Z5 was utilized for PL and TPC experiments.

The lengths of the nanowires were measured laterally, across the crack lines by tilting the sample and using the built-in system of the SEM unit to obtain the data. Z4 had the highest nanowire length (l) of ~ 1100 nm, followed by Z5 with 750 nm and finally Z3 had the nanowire length of ~ 600 nm. Z5 had the diameter, d ~ 40 nm, followed by Z4 with ~ 33 nm and by Z3 with ~ 24 nm. For the sample Z1, the length of the nanostructures were around l ~ 100 nm, with a diameter of d ~ 60 nm; whereas the nanoflower-like structures in Z2 consisted of petals of length l ~ 300 nm, with a diameter at the centre of d ~ 120 nm. All the lengths and diameters stated here are representative average lengths and diameters. It was observed that the nanowires were more aligned towards the vertical in the case of Z4. The tips of the nanowires were found to cluster together, as compared to the other samples where they were more oriented randomly towards the vertical.

SEM was also performed on the seeding layer. It exhibited a smoothly grained, compact surface with an average particle size of ~ 10 nm, with the exception of few larger particulates (30 - 40 nm) sitting on top of the surface. This might have been some larger particles sputtered from the target due to laser pulsing and also agglomerates of the smaller particles at the surface.

The XRD for a representative nanowire film (Fig. 2) indicated a sharp, intense peak due to (002) plane of hexagonal ZnO along with other very small peaks corresponding to (100), (101) and (103) planes of hexagonal ZnO (ICDD card no. 36-1451).

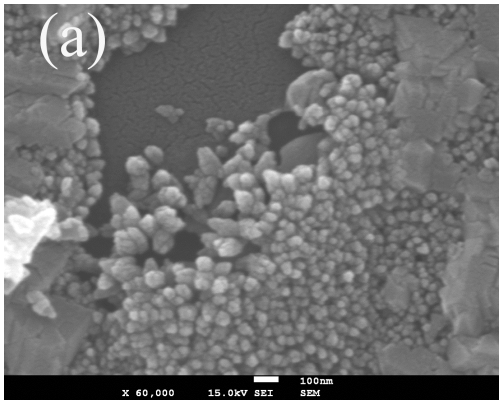

Fig. 1 Representative SEM images of as-deposited ZnO nanostructures: (a) Z1, (b) Z2, (c) Z3, (d) Z4 and (e) Z5 film.

The XRD thus confirmed highly c-axis oriented growth. The same c-axis orientation was followed for all the other samples.

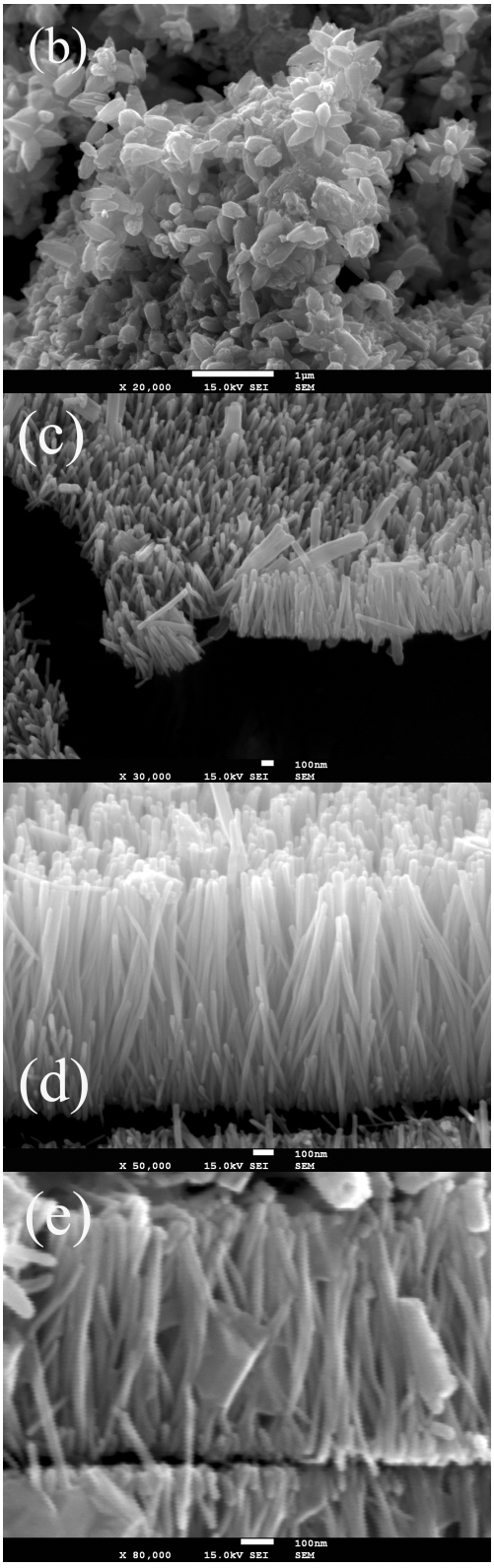

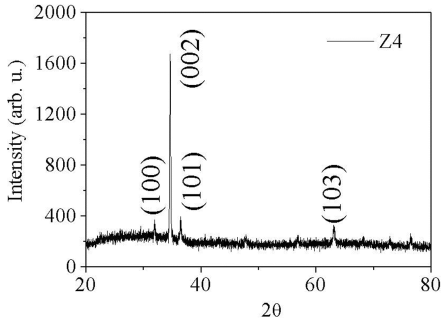

Fig. 2 XRD of representative ZnO nanowire film.

The band gap of the films were determined from the transmittance spectra (not shown here) by calculating the optical absorption coefficient [7], and was found to be between 3.2 eV to 3.3 eV for all the samples Z1 to Z5. They did not show too much variation for the five samples.

The PL measurements were performed at 300 K (room temperature). Our experimental setup was not sensitive enough to detect possible band edge luminescence (when measured without the 475 nm filter), whose intensity for our samples should be highly quenched due to their very small diameter. Fig. 3 shows the PL spectra for the samples Z3, Z4 and Z5 at 300 K. All the spectra were normalized to the highest intensity value. The spectra yielded broad yellow-orange luminescence peaks centred at ~ 2.1 eV. The sample Z4 having highest surface to volume ratio (aspect ratio), thereby highest density of surface defects, as compared to Z3 and Z5, had the yellow-orange band of highest intensity, followed by Z3 and Z5, in the order of their aspect ratios. The spectra for Z3 and Z5 seemed to be blue shifted with high asymmetry with a clear indication of a second peak at lower wavelengths. When deconvoluted, the spectrum for Z3 at 300 K revealed a peak at ~ 2.49 eV along with the peak ~ 2.08 eV, and the spectrum for Z5 also revealed a second peak at ~ 2.44 eV, along with a ~ 2.10 eV emission which is comparable to Z3. The blue shift in emission peaks (as a whole) for the Z3 and Z5 may thus be due to the appearance of these additional higher energy peaks (2.4 - 2.5 eV), which also pulled the centre towards higher energy.

The green band (around 2.4 - 2.5 eV) may be ascribed to the recombination of electrons with holes trapped in singly ionized oxygen vacancies (V_o^+) whereas the orange emission (around 2.1 eV) might be due to interstitial oxygen ions (O_i^-) [8].

TPC measurements were performed on the three samples Z3, Z4 and Z5, with vertically aligned nanowire structures. The sample Z4 was extremely highly resistive and did not yield any response at 15 V applied between the contacts. For the samples Z3 and Z5 decays could be measured in several time windows. It was found for both films, the decay had slow non-exponential power-law behaviour over several magnitudes of time. Fig. 4 shows a log-log plot of transient photocurrent decay vs. time for sample Z3.

Typically, for room temperature TPC measurements in wide bandgap semiconductors, having high band tailing or a large density of defects within the band gap, a sheet of charge is created on one side of the sample by strongly absorbed light. Charges of a given polarity drift through the sample to the opposite or adjacent collecting contact due to an external electric field. During the transit, carriers are frequently trapped in localized states below the band edges where they are immobile until reemitted to the bands. Some carriers, however, might disappear via recombination. Under the condition that carrier trapping is dominant, the photocurrent decay for these samples follow slow power law behaviour over several scales of time. This is the underlying theory of multiple trapping (MT) model [9], in disordered materials. In our case, the application of power-law equation for the photocurrent decay, $I = I_0 t^{\alpha}$ yield $\alpha \sim -0.40$ for Z3 and $\alpha \sim -0.63$ for Z5, respectively, from the log-log plot of the photocurrent decay vs. time. In other words, the decay corresponding to Z3 is slower than Z5, indicating larger density of surface states and defects within the forbidden gap, which contributes to the slower carrier mobility decay and hence a slower photo-response. The decay from sample Z5 contained a stronger contribution from recombination reflected by a faster decay process.

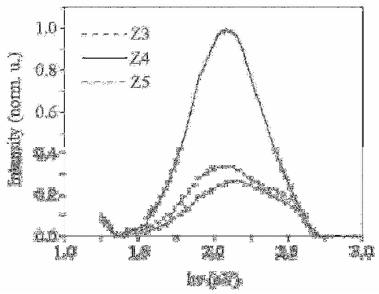

Fig. 3 Representative PL spectra at 300 K.

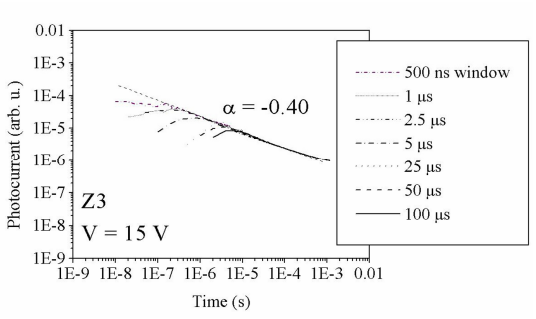

Fig. 4 Representative log-log plot of TPC for Z3.

4 CONCLUSION

ZnO nanowire thin films were deposited by a seeding layer mediated wet chemical process. The initial seeding layer with grain size ~ 10 nm was grown on glass substrate by PLD technique, upon which the ZnO nanostructures with diameters varying from 20 - 120 nm and lengths from 100 - 1100 nm were grown in aqueous medium using a magnetic stirrer at 333 K.

The PL of the samples indicated broad yellow-orange and green emission bands. The green band may have originated from oxygen vacancy related transitions, while the orange band arises from transitions due to interstitial oxygen ions. The large visible PL peaks and the absence of band-edge luminescence, which might be due to the size effect of the nanowires, indicate that the samples are highly defective with large density of surface states forming broad band tails within the forbidden gap, which governs the PL process for these samples.

Transient photocurrent decay measurements for the samples indicated slow, non-exponential, power law type decays over several magnitudes of time, characteristic of multiple trapping of carriers by the deep defects within the bandgap.

ACKNOWLEDGEMENT

One of the authors SRB wishes to thank FCT for granting a postdoctoral fellowship. He also wishes to express his gratitude towards S.V. College, West Bengal, India for their encouragement and support. JP and RA wish to thank FCT for grant of their fellowships. The work benefitted from funding of projects PTDC/FIS/108025/2008 and PTDC/CTM-CER/115085/2009.

REFERENCES

[1] Green M.A., 2007. Thin film solar cells: review of materials, technologies and commercial status, *J. Mater. Sci.: Mater. Electron.*, Vol. 18, No. 1, p. 15-19.

[2] Yeh N., Yeh P., 2013. Organic Solar cells: Their developments and potentials, *Renew. Sust. Energ. Rev.*, Vol. 21, p. 421-431.

[3] Arjunan T.V., Senthil T.S., 2013. Review: Dye sensitized solar cells, *Mater. Technol: Adv. Performance Mater.*, Vol. 28, No. 1-2, p. 9-14.

[4] Zhang Q., Yodyingyong S., Xi J., Myers D., Cao G., 2012. Oxide nanowires for solar cell applications, Nanoscale, Vol. 4, No. 5, p. 1436-1445.

[5] Kumar B., Kim S.-W., 2012. Energy harvesting based on semiconducting piezoelectric ZnO nanostructures, *Nano Energy*, Vol. 1, No. 3, p. 342-355.

[6] Briscoe J., Bilotti E., Dunn S., 2012. Measured efficiency of a ZnO nanostructured diode piezoelectric energy harvesting device, *Appl. Phys. Lett.*, Vol. 101, No. 9, p. 093902.

[7] Bhattacharyya S.R., Majumder S., 2010, Synthesis of Al doped ZnO films by sol-gel technique, *Funct. Mater. Lett.* Vol. 3, No. 2, p. 111-114.

[8] Greene L.E., Law M., Goldberger J., Kim F., Johnson J.C., Zhang Y., Saykally R.J., Yang P., 2003. Low-temperature wafer-scale production of ZnO nanowire arrays, *Angew. Chem. Int. Ed.*, Vol. 42, No. 26, p. 3031-3034.

[9] Tiedje T., Rose A., 1981. A physical interpretation of dispersive transport in disordered semiconductors, *Solid State Commun.*, Vol. 37, No. 1, p. 49-52.